Freshwater alga *Raphidocelis subcapitata* undergoes metabolomic changes in response to electrostatic adhesion by micrometer-sized nylon 6 particles

Satomi Mizukami Murata (s-murata@pwri.go.jp)
Public Works Research Institute: Dokuritsu Gyosei Hojin Doboku Kenkyujo
Yuji Suzuki
Public Works Research Institute: Dokuritsu Gyosei Hojin Doboku Kenkyujo
Kensuke Sakurai
Public Works Research Institute: Dokuritsu Gyosei Hojin Doboku Kenkyujo
Hiromasa Yamashita
Public Works Research Institute: Dokuritsu Gyosei Hojin Doboku Kenkyujo

Research Article

Keywords: Powdered nylon 6, Raphidocelis subcapitata, Growth inhibition, Electrostatic adhesion, Metabolomic analysis, Amino acid catabolic pathway, γ-glutamyl cycle

Posted Date: April 30th, 2021

DOI: https://doi.org/10.21203/rs.3.rs-343076/v1

Version of Record: A version of this preprint was published at Environmental Science and Pollution Research on July 8th, 2021. See the published version at https://doi.org/10.1007/s11356-021-15300-8.

Abstract

Nylon powders are a type of microplastic (MP) used in personal care products such as cosmetics and sunscreens. To determine the effects of nylon on freshwater microalgae, we investigated the effects of two types of micrometer-sized nylons, i.e., powdered nylon 6 (Ny6-P) and nylon 12 (Ny12), and four other micrometer-sized MPs, i.e., low-density polyethylene, polyethylene terephthalate, polystyrene, and ultra-high-molecular-weight polyethylene, on the microalga *Raphidocelis subcapitata*. The results showed that Ny6-P inhibited *R. subcapitata* growth more than the other MPs; *R. subcapitata* growth was inhibited by 54.2% with 6.25 mg/L Ny6-P compared with the control. Ny6-P in the culture media adhered *R. subcapitata* cells electrostatically, which disrupted growth and photosynthesis. Metabolomic analysis revealed that many metabolites related to the amino acid catabolic pathway and γ-glutamyl cycle were induced, which might reflect responses to avoid starvation and oxidative stress. Our study provides important information on the effects of Ny6-P on algae in freshwater environments.

1. Introduction

Since the 1950s, the production and use of plastics has increased globally, which has affected the environment, especially in terms of increased amounts of microplastics (MPs) released into aquatic environments (Monteleone et al. 2019). MPs are defined as plastic particles sized < 5 mm and can be further categorized based on the production process. Primary MPs are produced as plastic resin pellets or granules that are often added to personal care products, which may flow into aquatic environments mainly via domestic wastewater (Thompson et al. 2004; Mintenig et al. 2017). Secondary MPs are generated as a result of the degradation of larger plastic products over time due to physical, biological, and chemical weathering processes (Li et al. 2016). The use of plastics has resulted in MP contamination in aquatic environments and is drawing attention worldwide. In addition to their presence in marine environments, MPs have been detected at concentrations ranging from 0.00297 to 2.58 g/L in freshwater environments, including rivers, lakes, and wastewater treatment plants, in North America, Asia, Europe, and Australia (Eerkes-Medrano et al. 2015; Rezania et al. 2018; Li et al. 2019). Moreover, various types of MP polymers, such as polyamide (PA), polyethylene (PE), PE terephthalate (PET), polypropylene (PP), and polystyrene (PS), have been detected in these regions (Li et al. 2019; Rezania et al. 2018).

Understanding the effects of MPs on microalgae is essential because microalgae comprise the base of the food chain in aquatic environments. Many studies have investigated the effects of MPs on freshwater and marine algae in recent years (Bhattacharya et al. 2010; Besseling et al. 2014; Davarpanah and Guilhermino 2015; Sjollema et al. 2016; Bergami et al. 2017; Zhang et al. 2017; Canniff and Hoang 2018; Chae et al. 2018; Mao et al. 2018; Prata et al. 2019; Yi et al. 2019). Most of the researches have focused on the effects of PS on algal cells (Bhattacharya et al. 2010; Casado et al. 2013; Besseling et al. 2014; Sjollema et al. 2016; Bergami et al. 2017; Chae et al. 2018; Yi et al. 2019). Nanometer-sized PS particles have been reported to inhibit algal photosynthesis and growth, whereas micrometer-sized PS particles did not pose such effects (Besseling et al. 2014; Sjollema et al. 2016; Yi et al. 2019). Moreover, aggregation of positively charged PS particles was observed when algal cells co-existed, which induced structural damage and oxidative stress in algae; these effects were greater than those of negatively charged PS particles (Bhattacharya et al. 2010; Bergami et al. 2017). The effects of different plastic types other than PS on algal cells have also been reported. Micrometer-sized polyvinyl chloride (PVC) was shown to inhibit microalgal growth via heteroaggregation, which resulted in physical damage to the cells (Zhang et al. 2017; Song et al. 2020). Relatively large-sized PE particles (diameter, 63–75 μm) were reported to enhance algal growth, whereas small-sized PE particles (1–5 μm) had no effects on algae (Davarpanah and Guilhermino 2015; Canniff and Hoang 2018). However, comparing the toxic effects of different plastic types is difficult because the experimental conditions and tested algae species varied among studies. Additionally, previous reports focused on nanometer-sized particles, which are smaller than microalgae. Micrometer-sized MPs, which are larger than

algal cells, are commonly found in aquatic environments; thus, the effects of micrometer-sized MPs on algal cells should be investigated (Eerkes-Medrano et al. 2015; Rezania et al. 2018; Li et al. 2019).

Polyamides (nylon) particles are used in personal care products such as face powder and eyeshadow as opacifying and skin-improving agents (Timm et al. 2011; Burnett et al. 2014). Thus, nylon MPs can be introduced into freshwater environments through human activities such as swimming and also the influx of domestic wastewater. Nylon particles are one of the most common MPs detected in aquatic environments, and the impact of nylon on algal cells cannot be ignored (Erni-Cassola et al. 2017; Mintenig et al. 2017; Li et al. 2019; Scopetani et al. 2019; Yan et al. 2019). Micrometer-sized PA particles have been detected in sewage effluents from wastewater treatment plants and freshwater fishes (Mintenig et al. 2017; Wagner et al. 2019). However, the effects of nylon on algal cells have not yet been elucidated.

The aim of this study was to determine the effect of nylons on the freshwater microalga *Raphidocelis subcapitata*. *R. subcapitata* is widely distributed in freshwater environments and serves as a typical model phytoplankton species for toxicology testing (OECD guidelines, 2011). To compare the effects of nylon and other MPs on algal cells, we examined the effects of seven types of MPs—nylon 6 (Ny6), nylon 12 (Ny12), low-density PE (LDPE), PET, PP, PS, and ultra-high-molecular-weight-PE (UHPE)—on *R. subcapitata* growth and photosynthesis. Many everyday items are produced from these materials (Li et al. 2016); styrene foams used for food packaging are composed of PS, shopping bags are composed of LDPE, items such as skis and climbing ropes are composed of UHPE, and bottles and lids are composed of PET and PP, respectively. Ny6 and Ny12 are used extensively to produce textile fibers in addition to personal care products. In this study, we evaluated powdered MPs [LDPE, powdered Ny6 (Ny6-P), Ny12, PET, PS, and UHPE] and granule-type MPs [granule Ny6 (Ny6-G) and PP]. We exposed *R. subcapitata* cells to each type of MP and examined the effect on growth and photosynthesis. The adhesion of *R. subcapitata* by Ny6-P was evaluated by microscopic observation and by measuring electronic potentials. In addition, we employed metabolomic analysis, which is emerging as a powerful omics tool to elucidate organism response mechanisms under stress conditions. Many studies have examined the effects of MPs on organisms such as fish, shellfish, and plants, but few have employed metabolomics on alga (Qiao et al. 2019; Ding et al. 2020; Wu et al. 2020; Teng et al. 2021). Here, we performed metabolomic analysis to expand our understanding of the biochemical mechanisms of *R. subcapitata* responses to Ny6-P adhesion.

2. Materials And Methods

2.1. MPs

Six powdered MPs (LDPE, Ny6-P, Ny12, PET, PS, and UHPE) were purchased from Goodfellow Cambridge Ltd. (Japan) for this experiment. The maximum particle size of Ny6-P and Ny12 was 50 μm (average diameters: Ny6, 15–20 μm; Ny12, 25–30 μm). Four MPs (LDPE, PET, PS, and UHPE; diameter < 300 μm) were used after fractionation with a 53-μm stainless-steel mesh sieve. Two granule-type MPs were used, Ny6-G and PP (average diameter: 3 mm). All MPs were white in color and contained no additives.

2.2. Test species and culture conditions

The green alga *R. subcapitata* (NIES-35) was obtained from the Microbial Culture Collection of the National Institute for Environmental Studies (NIES) of Japan. *R. subcapitata* was cultured in AAP medium sterilized by membrane filtration (0.22-μm pore size) in a sterilized flask (OECD guidelines, 2011). Algal cells were cultured at 25 ± 1°C on a rotating shaking device at 100 rpm (Taitec Co., NR-80, Japan) in an incubator under white fluorescent light [3,000 Lux, measured using an illuminance meter (mobiken Lx2, Sanwa Co., Japan)] with a 16-h/8-h light/dark cycle. Algal cells were subcultured every week. Additionally, *R. subcapitata* was cultured in C medium under the same culture conditions to yield a higher concentration of cells for the algal adhesion tests and metabolomic analysis (NIES collection, 2001). Algal cells were subcultured every 2 weeks.

2.3. Algal growth and photosynthesis inhibition test

Four Ny6-P concentrations (6.25, 12.5, 25, and 50 mg/L) and three Ny12 concentrations (150, 350, and 750 mg/L) were tested. Four powdered MPs (LDPE, PET, PS, and UHPE) were examined at a concentration of 750 mg/L. The granule-type MPs were tested at a concentration of 7,500 mg/L (13 Ny6-G particles, 6 PP particles) because the particle weights of Ny6-G and PP were approximately 11.5 mg and 24.5 mg, respectively. *R. subcapitata* cells were incubated for 72 h until reaching log-phase growth and then added to a flask containing AAP medium at an initial cell density of 1×10^4 cells/mL. The samples were cultured in an incubator for 72 h at 25 ± 1°C under constant illumination at 4,000 Lux on a rotating shaking device at 100 rpm. The flasks were positioned randomly for incubation. Samples with only algal cells (without MPs) were used as the control. In the Ny6-P and Ny12 treatments, algal cell numbers were determined every 24 h using a cell counter (CDA-1000B, Sysmex Co., Japan). In the LDPE, PET, PS, UHPE, Ny6-G, and PP treatments, algal cell numbers were determined after 72 h. For the photosynthesis analysis, the chlorophyll-a (Chl-a) contents of each flask were measured after 72 h of exposure. All experiments were performed in triplicate.

2.4. Measurement of Chl-a content

After exposure of *R. subcapitata* to MPs for 72 h, the culture solutions were filtered (GF/C, Whatman) and the filter papers were stored at − 30°C until further analyses. Filtered samples were ground using a mortar with 10 mL of acetone (90% concentration with Milli-Q water, Fujifilm Wako Pure Chemical Co., Ltd., Japan) and stored at 4°C overnight to extract Chl-a. Supernatants were obtained by centrifuging twice at 1,500 × *g* for 10 min. The Chl-a content was determined using a ultraviolet–visible recording spectrophotometer (UV-160, Shimadzu Inc., Japan) based on the absorption technique described by Lorenzen (1967). The absorbances of the extracted samples were measured at 665 nm and 750 nm to determine the Chl-a content.

2.5. Nylon adhesion tests

The Ny6-P EC_{50} for *R. subcapitata* cells (1×10^4 cells/mL) was calculated as 5–6 mg/L using data shown in Fig. 1-a (6.25 mg/L Ny6-P reduced *R. subcapitata* growth by 54.2%). Based on these results, algal cell and nylon concentrations approximately 100-fold higher were used in the adhesion experiment to enable naked-eye observations. Ny6-P or Ny12 (500 mg/L) was added to the C medium, and algal cell culture solution was added to each flask at an initial cell density of 1×10^6 cells/mL. Each sample was incubated at 25 ± 1°C under constant illumination (4,000 Lux) on a rotating shaking device at 100 rpm. Algal cells without MPs were used as the control. The number of particles in the supernatant (A), including algal cells and nylon particles, was measured at five time points (0, 30, 90, 240, and 300 min) using a cell counter. The number of nylon particles in the medium (B) was also measured at each time point. The number of algal cells in the supernatant was calculated by subtracting (A) from (B). After incubation for 300 min, precipitates in each flask were observed using an optical microscope (BX51, Olympus Co., Japan). All experiments were performed in triplicate.

2.6. Zeta potential measurement

R. subcapitata cells (8×10^4 cells/mL) and 5 mg/L Ny6-P in AAP medium were stirred for 1 min to allow Ny6-P adhesion to *R. subcapitata* cells. After stirring, the samples were allowed to stand for 1 min, and the zeta potential was then measured. Approximately 1 mL of each sample was injected into the cuvette for zeta potential analysis, which was conducted at 20°C using a Zeta Potential and Submicron Particle Size Analyzer (Delsa™Nano HC, Beckman Coulter Inc., Japan). All experiments were performed in triplicate.

2.7. Metabolomic analysis

R. subcapitata cells (1×10^4 cells/mL) were treated with Ny6-P (6 mg/L) in C medium and incubated at 25 ± 1°C under constant illumination (4,000 Lux) on a rotating shaking device at 100 rpm. After 0, 6, and 24 h of treatment, algal cells

(3×10^7 cells) were collected by filtration using 1.0-μm pore-sized Omnipore™ membrane filters (hydrophilic PTFE, Merck Millipore, UK) and washed twice with Milli-Q water. The filters were then soaked in 2.0 mL of methanol containing Milli-Q water and internal standards (H3304-1002, Human Metabolome Technologies [HMT], Japan) and ultrasonicated for 30 s. Cell suspensions were stored at − 80°C until further analysis. The extract was obtained with cell disruption and centrifuged at 2,300 × *g* at 4°C for 5 min. Then, 700 μL of the upper aqueous layer was centrifugally filtered through a Millipore 5-kDa cutoff filter at 9,100 × *g* at 4°C for 120 min to remove proteins. The filtrate was concentrated by centrifugation and resuspended in 50 μL of Milli-Q water for capillary electrophoresis time-of-flight mass spectrometry (CE-TOFMS) analysis.

Metabolome analysis was performed using CE-TOFMS (Ohashi et al. 2008; Ooga et al. 2011). Briefly, CE-TOFMS analysis was conducted using an Agilent capillary electrophoresis system equipped with an Agilent 6210 time-of-flight mass spectrometer (Agilent Technologies, Germany). The systems were controlled using Agilent G2201AA ChemStation software version B.03.01 for CE (Agilent Technologies) and connected by a fused silica capillary tube (50 μm i.d. × 80 cm total length) with commercial electrophoresis buffers (H3301-1001 and I3302-1023 for cation and anion analyses, respectively, HMT) as the electrolyte. The spectrometer was scanned from m/z 50 to 1,000. Peaks were extracted using MasterHands automatic integration software (Keio University, Japan; Sugimoto et al. 2009) and MassHunter Quantitative Analysis B.04.00 (Agilent Technologies) to obtain m/z, peak area, and migration time (MT). Signal peaks were annotated according to the metabolite database based on their m/z values and MTs. Annotated peak areas were then normalized based on the internal standard and sample amounts to obtain relative levels of each metabolite. Principal component analysis was performed using PeakStat and SampleStat which are HMT's proprietary softwares. Algal cells without MPs were used as the control. The time-course experiment was performed once.

2.8. Statistical analysis

Data were expressed as the mean ± standard deviation of three independent experiments. Statistical differences between control and treated algal cells were determined using *t*-tests. Significance levels were set at $P < 0.05$ and $P < 0.01$.

3. Results And Discussion

3.1. Effects of nylons on R. subcapitata

The effects of nylon on *R. subcapitata* were evaluated using two types of nylons, Ny6-P and Ny12. Figure 1-a and b shows *R. subcapitata* growth under various Ny6-P concentrations. Algal growth was inhibited with increasing Ny6-P concentration (Fig. 1-a). At 72h passed, the number of algal cells observed under the condition with 6.25 mg/L of Ny6-P was 54% less than that observed under the control condition, although the difference was not statistically significant ($P = 0.06$, Fig. 1-b). Interestingly, the number of algal cells decreased under the 12.5, 25, and 50 mg/L Ny6-P treatments; after 72 h, the number of cells was reduced by 88.3%, 76.7%, and 95.0%, respectively, compared with the 0h control (1×10^4 cells/mL). The Chl-a contents of *R. subcapitata* treated with Ny6-P were also examined (Fig. 1-c). The Chl-a contents decreased with increasing Ny6-P concentration, following a similar trend as algal cell growth; a small amount of Chl-a was detected in *R. subcapitata* cells treated with Ny6-P concentrations > 12.5 mg/L (inhibition rate: 95.4%; $P < 0.01$). These results demonstrate that Ny6-P has the capacity to inhibit *R. subcapitata* cell growth.

Figure 2 shows the growth of *R. subcapitata* cells treated with Ny12. Algal cell growth was inhibited with increasing Ny12 concentration, but higher concentration of Ny12 (more than 350 mg/L) was required to inhibit cell growth compared with 6.25 mg/L of Ny6-P (Fig. 2-a). The number of algal cells was reduced by 20.4%, 70.9%, and 63.8% after 72 h of treatment with 150, 350, and 750 mg/L Ny12, respectively, compared with the control. Similarly, the Chl-a content decreased with increasing Ny12 concentration (Fig. 2-b). After 72 h, the *R. subcapitata* Chl-a content in the 350

mg/L Ny12 treatment was reduced by 49.2% compared with that in the control ($P < 0.01$). These results show that Ny6-P has a greater capacity to inhibit *R. subcapitata* growth than Ny12. Moreover, Ny6-P particles sank to the bottom of the flasks more easily than Ny12 particles (data not shown). Ny6-P was uniformly dispersed in the medium, whereas Ny12 formed uneven aggregates after 72 h of treatment. These differences in dispersion may reflect differences in inhibitory effects on *R. subcapitata* among Ny6-P and Ny12.

The effects of granule-type MPs (Ny6-G and PP; diameter, 3 mm) on *R. subcapitata* were investigated (Supplementary data Fig. S1). Under the experimental conditions, no significant decreases in growth and photosynthesis (Chl-a content) were observed in the Ny6-G or PP treatment, even at the highest concentration (7,500 mg/L). These results suggest that millimeter-sized MPs do not inhibit *R. subcapitata* growth. Block-type PVC (1 mm) did not affect *Skeletonema costatum* growth compared with powdered PVC (1 μm) (Zhang et al. 2017). Micrometer-sized PS (5–6 μm) did not affect *Chlorella pyrenoidosa* growth compared with nanometer-sized PS (0.55 μm) (Sojollema et al. 2016; Yi et al. 2019). Our results also indicate that the particle size of Ny6 (powder or granule) is an important indicator of the potential effects on algal growth.

3.2. Effects of four types of MPs on R. subcapitata

To compare the effects of nylons and other MPs on *R. subcapitata*, we examined the effects of powdered LDPE, PET, PS, and UHPE on *R. subcapitata*. Figure 3-a and -b shows the ratios of cell densities and Chl-a contents of *R. subcapitata* treated with each MP compared with the corresponding control conditions. PET, PS, and UHPE did not significantly affect *R. subcapitata* growth or Chl-a content, even at the highest concentration of 750 mg/L. After 72 h, only LDPE decreased the number of algal cells and Chl-a content by 50.4% and 27.9%, respectively, although the differences were not statistically significant. Our results indicate that these MPs had limited effects on *R. subcapitata* growth and photosynthesis. Among all conducted experimental conditions, Ny6-P had the greatest inhibitory effect on *R. subcapitata* growth, followed by Ny12, LDPE, PS, UHPE, and PET.

Previous studies have reported that micrometer-sized MPs affect algal growth (Table 1). For example, PVC had higher capacity to inhibit algal growth; 50 mg/L PVC (1 μm) inhibited the growth of *S. costatum* by 39.7% and 200 mg/L PVC (74 μm) inhibited the growth of *Phaeodactylum tricornutum* MASCC-0025 by 21.2% after 96 h of exposure (Zhang et al. 2017; Zhu et al. 2019; Song et al. 2020). Moreover, 1-μm PS (100 mg/L) inhibited the growth of *C. pyrenoidosa* by 38.1% after 22 days of exposure (Mao et al. 2018). In contrast, PE promoted the growth of *Chlorella* sp. and *R. subcapitata* (Canniff and Hoang, 2018; Song et al. 2020). Compared with the previous reports, our results suggest that micrometer-sized Ny6-P has a higher capacity to inhibit algal growth than other MPs, although no direct comparisons could be made because the tested algal species and MP size differed among studies.

Table 1
Effects of micrometer-sized microplastics on algae

Microplastic*	Size (μm)	Maximum concentration (mg)	Environment	Alga	Exposure time	Effects	Reference
PS	6	250	Salt water	*Dunaliella tertiolecta*	72 h	No effect	Sjollema et al. 2016
PS	5	60	Freshwater	*Chlorella pyrenoidosa*	96 h	No effect	Yi et al. 2019
PS	1	100	Freshwater	*Chlorella pyrenoidosa*	22 d	Growth inhibition	Mao at al. 2018
PVC	1	50	Salt water	*Skeletonema costatum*	96 h	Growth inhibition	Zhang et al. 2017
PVC	1000	2000	Salt water	*Skeletonema costatum*	96 h	No effect	
PE, PET, and PVC	74	200	Freshwater	*Chlorella sp. L38*	96 h	Growth promotion	Song et al. 2020
PE, PET, PP, and PVC	74	200	Salt water	*Phaeodactylum tricornutum MASCC-0025*	96 h	Growth inhibition	
PE, PS, and PVC	74	100	Salt water	*Skeletonema costatum*	96 h	Growth inhibition	Zhu et al. 2019
PE	130	36–75	Freshwater	*Raphidocelis subcapitata*	5 d	Growth promotion	Canniff and Hong 2018
PP	400–1000	400	Freshwater	*Chlamydomonas reinhardtii*	78 d	Growth inhibition	Lagarde et al. 2016
HDPE	400–1000	400	Freshwater	*Chlamydomonas reinhardtii*	78 d	No effect	

* high density PE, HDPE; polyethylene, PE; PE terephthalate, PET; polypropylene, PP; polystyrene, PS; polyvinyl chloride, PVC

3.3. Adhesion of R. subcapitata cells and nylon particles

Nylons posed more inhibitory effects on *R. subcapitata* growth than the four other types of MPs. To gain deeper understanding of the phenomena underlying this observation, we performed further experiments using Ny6-P and Ny12. Figure 4-a shows the number of algal cells in the supernatant of media treated with each nylon. The number of algal cells immediately decreased with Ny6-P treatment, and the number of cells was reduced by 87% compared with the control after 6 h of incubation. In this treatment, particles of green-colored Ny6-P, which adhered many algal cells, were observed at the bottom of the flask, whereas the supernatant was transparent (Fig. <link rid="fig4">4</link>-c and 4-d). In the Ny12 treatment, the number of algal cells gradually decreased with time; the number of cells was reduced by 42.3% after 6 h of incubation (Fig. 4-a). Ny12 precipitates were also observed at the bottom of flasks with slightly green-colored (data not shown). These results indicate that Ny6-P has a higher capacity to cause adhesive interaction with *R. subcapitata* cells than Ny12. Under the experimental conditions, one Ny6-P particle was estimated to attract 7.4 algal cells to adhere after 300 min of incubation.

Nanometer-sized MPs, including PS and PVC, have been reported to adsorb to algal cell surfaces (Zhang et al. 2017; Mao et al. 2018; Yi et al. 2019). Our results show that micrometer-sized Ny6-P particles possess the ability to adhere *R. subcapitata* cells. Figure 4-b shows the zeta potentials of Ny6-P and *R. subcapitata* cells, which were measured to quantify the adhesion characteristics of Ny6-P to *R. subcapitata* cells. Ny6-P and *R. subcapitata* cells in media had zeta potentials of 13.0 mV and − 36.0 mV, respectively. After interaction with Ny6-P, *R. subcapitata* cells (*R. subcapitata* + Ny6-P) exhibited an increased zeta potential (− 26.5 mV). PA (nylon 6, 6) is known to be positively charged, whereas typical plastic materials such as PE and PS tend to be negatively charged in triboelectric series (Liu et al. 2015; Kim et al. 2017). Algal cells are also known to be negatively charged (Ewerts et al. 2017). It has been demonstrated that positively charged PS particles (20–50 nm) have a higher binding affinity toward algal cells, which produces a greater effect on the cells than negatively charged PS particles (Bergami et al. 2017; Nolte et al. 2017; Bhattacharya et al. 2010). Based on these results, the present study suggests that positively charged Ny6-P has a binding affinity toward negatively charged *R. subcapitata* and that electrostatic adhesive interaction between them inhibits algal cell growth. These findings are consistent with the observed decrease in the number of *R. subcapitata* cells treated with Ny6-P (Fig. 1-a).

3.4. Global metabolomic analysis of R. subcapitata treated with Ny6-P

To elucidate the biochemical mechanism of *R. subcapitata* response to adhesion by Ny6-P, metabolomics analysis was performed using CE-TOFMS. The analysis showed the presence of 177 compounds as primary metabolites (Table S1), which led to the detection of 89 signals in cation mode and 88 signals in anion mode. Figure 5-a shows the PCA plot of *R. subcapitata* metabolites with and without Ny6-P treatment. As shown in the plot, algal cells treated with Ny6-P were clearly separated from the control group. The first principal component (PC1) accounted for 42.1% of the variation, showing the variation in metabolites resulting from the effects of Ny6-P on *R. subcapitata*, and the second principal component (PC2) accounted for 24.4% of the variation, showing the variation in metabolites during *R. subcapitata* growth. In particular, metabolites related to five amino acids [phenylalanine (Phe), glycine (Gly), methionine (Met), histidine (His), and isoleucine (Ile)] and three gamma-glutamyl (γ-Glu) amino acids [γ-Glu-asparagine (Asn), γ-Glu-His, and γ-Glu-lysine (Lys)_divalent] exhibited the 10 highest factor loadings in PC1 (Table S2). Figure 5-b shows the expressed metabolites (19 induced and 5 repressed) in *R. subcapitata* cells treated with Ny6-P for 6 and 24 h. High accumulation of amino acids was observed as an important adjustment of the organism following treatment with Ny6-P. Twelve amino acids, i.e., alanine (Ala), arginine (Arg), His, Ile, leucine (Leu), Met, Phe, proline (Pro), serine (Ser), threonine (Thr), tyrosine (Tyr), and valine (Val), were detected in 19 metabolites with increased expression. During 24h exposure, amino acid contents mostly increased with time. At 24h passed, particularly, His, Phe, and Pro exhibited 8.21-, 6.72-, and 6.74-fold increases in concentration that observed under the control condition, respectively.

In general, algae generate energy for growth by photosynthetic carbon assimilation under photoirradiation. In contrast, algae accumulate free amino acids as energy sources via autophagy systems under stress conditions such as starvation and dark condition as well as plants and yeast (Izumi et al. 2013; Hildebrandt et al. 2015; Hirota et al. 2018; Mubeen et al. 2018). MPs have been demonstrated to decrease chlorophyll contents in algal cells (Fig. 1-c; Song et al. 2020; Zhan et al. 2017). Decreases in φPSII activity were also reported in algae treated with MPs (Zhan et al. 2017; Sjollema et al. 2016). The adhesion of MPs onto the surface of algal cells may shield light and impede nutrient intake, thereby disrupting normal photosynthesis and respiration processes. Our metabolomic results suggested that the energy availability was changing from photosynthetic carbon assimilation to amino acid catabolic pathway in *R. subcapitata* after adhesion of Ny6-P particles. Among the repressed metabolites, three amino acids involved in energy synthesis via the tricarboxylic acid cycle were detected (Fig. 5-b). At 24h passed, citric acid, malic acid, and adenosine triphosphate (ATP) exhibited 0.4-, 0.2-, and 0.6-fold decreases in concentration that observed under the control condition, respectively. These results may reflect energy starvation resulting from photosynthesis interference.

MPs have been demonstrated to induce oxidative stress in algae in addition to causing physical damage (Bhattacharya et al. 2010; Mao et al. 2018; Song et al. 2020). Adsorption of nanometer-sized and positively charged PS particles stimulated reactive oxygen species (ROS) production in *Chlorella* and *Scenedesmus* (Bhattacharya et al. 2010). Micrometer-sized PP, PE, PET, and PVC also produced signs of oxidative stress in *Chlorella* sp. and *P. tricornutum*, as detected by measuring malondialdehyde and superoxide dismutase concentrations (Song et al. 2020). Furthermore, PS beads induced electron accumulation from damaged chloroplasts, which caused oxidative stress in *C. pyrenoidosa* (Mao et al. 2018). The γ-glutamyl cycle is an antioxidative system that protects against ROS accumulation (Masi et al. 2015; Bachhawat et al. 2018). The γ-glutamyl cycle is responsible for the biosynthesis and utilization of glutathione by amino acid transport systems and uses ATP as energy. As shown in Fig. 6, most metabolites related to the γ-glutamyl cycle were induced with time, although metabolites related to amino acids overlapped in the amino acid catabolic pathway. Only γ-Glu-Arg-divalent was detected as a γ-Glu-amino acid at 6 and 24 h, although four other γ-Glu-amino acids, γ-Glu-Lys divalent, γ-Glu-Phe, γ-Glu-tryptophan (Trp), and γ-Glu-Tyr, were found to be accumulated at 24 h (Fig. 6). These results indicate that induction of the γ-glutamyl cycle may provide protection from oxidative stress in *R. subcapitata* cells adhered on Ny6-P. Some metabolites related to oxidative stress were also detected (Fig. S2). Two metabolites, citrulline and γ-aminobutyric acid (GABA), were accumulated at 6 and 24 h (Fig. 5-b). Citrulline protects DNA and enzymes from oxidative injuries, and GABA restricts ROS accumulation in plants (Akashi et al. 2001, Roberto et al. 2019). Four other metabolites related to oxidative stress in plants, i.e., cadaverine, dopamine, methionine sulfoxide, and 5-oxoproline, were also detected after treatment for 24 h (Aronova et al. 2005; Jacques et al. 2015; Liu et al. 2020; Ohtsu et al. 2008; Shevyakova et al. 2001; Fig. S2). Our results suggest that oxidative stress, though not observed directly, was produced in *R. subcapitata* cells adsorbed by Ny6-P, which responded via the activation of antioxidant systems, such as the γ-glutamyl cycle.

4. Conclusion

This study demonstrated that Ny6-P had the highest ability to inhibit *R. subcapitata* photosynthesis and growth among all tested MPs, including Ny12, LDPE, PET, PS, and UHPE. Our results showed that micrometer-sized MPs had effects on *R. subcapitata* cells, and these effects were dependent upon the chemical compositions of the MPs. Figure 7 illustrates the response of *R. subcapitata* to treatment with Ny6-P. When Ny6-P was added to the culture solution, *R. subcapitata* electrostatically adhered to the surface of Ny6-P particles. These effects may inhibit *R. subcapitata* photosynthesis and growth by shielding light and impeding nutrient intake. Under this condition, it was indicated that the amino acid catabolic pathway is induced in *R. subcapitata*, which may be an avoidance response to starvation. Ny6-P may also cause oxidative stress in *R. subcapitata* cells. *R. subcapitata* induced several metabolites related to oxidative stress, including those of the γ-glutamyl cycle, which may be to reduce the stress. These findings provide novel insights into the toxicity mechanism of Ny6-P in freshwater algae.

Declarations

Acknowledgments

We would like to thank Michiko Okubo and Mie Harada for technical assistance.

Authors' contributions

Conceptualization and design of study, Methodology, Investigation, Writing–Original draft preparation: SM; Conceptualization and design of study, Supervision, Writing–Reviewing and Editing: YS and HM; Design of study and analysis of zeta potential: KS. All authors read and approved the final manuscript.

Funding

This work was partially supported by JSPS KAKENHI [grant number 18K04418].

Availability of data and materials

Data used within this research are available upon request from the corresponding author.

Competing interests

The authors declare that they have no conflict of interest.

Ethical approval

Not applicable.

Consent to participate

Not applicable.

Consent to publish

Not applicable.

References

Akashi K, Miyake C, Yokota A (2001) Citrulline, a novel compatible solute in drought-tolerant wild watermelon leaves, is an efficient hydroxyl radical scavenger. FEBS Lett 508:438–442. https://doi.10.1016/s0014-5793(01)03123-4

Aronova EE, Sheviakova NI, Stetsenko LA, Kuznetsov VV (2005) Cadaverine-induced induction of superoxide dismutase gene expression in *Mesembryanthemum crystallinum* L. Dokl Biol Sci 403:257–259.

Bachhawat AK, Yadav S (2018) The glutathione cycle: Glutathione metabolism beyond the gamma-glutamyl cycle. IUBMB Life 70:585–592. https://doi.10.1002/iub.1756

Bergami E, Pugnalini S, Vannuccini ML, Manfra L, Faleri C, Savorelli F, Dawson KA, Corsi I (2017) Long-term toxicity of surface-charged polystyrene nanoplastics to marine planktonic species *Dunaliella tertiolecta* and *Artemia franciscana*. Aquat Toxicol 189:159–169. https://doi.org/10.1016/j.aquatox.2017.06.008

Besseling E, Wang B, Lürling M, Koelmans AA (2014) Nanoplastic affects growth of *S. obliquus* and reproduction of *D. magna*. Environ Sci Technol 48:12336–12343. https://doi.org/10.1021/es503001d

Bhattacharya P, Lin S, Turner JP, Ke PC (2010) Physical adsorption of charged plastic nanoparticles affects algal photosynthesis. J Phys Chem C 114:16556–16561. https://doi.org/10.1021/jp1054759

Burnett C, Heldreth B, Bergfeld WF, Belsito DV, Hill RA, Klaassen CD, Liebler DC, Marks JG Jr, Shank RC, Slaga TJ, Snyder PW, Andersen FA (2014) Safety assessment of nylon as used in cosmetics. Int J Toxicol 33 (4 Suppl):47S–60S. https://doi.org/10.1177%2F1091581814563524

Canniff PM, Hoang TC (2018) Microplastic ingestion by *Daphnia magna* and its enhancement on algal growth. Sci Total Environ 633:500–507. https://doi.org/10.1016/j.scitotenv.2018.03.176

Casado MP, Macken A, Byrne HJ (2013) Ecotoxicological assessment of silica and polystyrene nanoparticles assessed by a multitrophic test battery. Environ Int 51:97–105. https://doi.10.1016/j.envint.2012.11.001

Chae Y, Kim D, Kim SW, An YJ (2018) Trophic transfer and individual impact of nano-sized polystyrene in a four-species freshwater food chain. Sci Rep 8:284. https://doi.10.1038/s41598-017-18849-y

Davarpanah E, Guilhermino L (2015) Single and combined effects of microplastics and copper on the population growth of the marine microalgae *Tetraselmis chuii*. Estuar Coast Shelf Sci 167, Part A:269–275.

Ding J, Huang Y, Liu S, Zhang S, Zou H, Wang Z, Zhu W, Geng J (2020) Toxicological effects of nano- and micro-polystyrene plastics on red tilapia: Are larger plastic particles more harmless? J Hazard Mater 396:122693. http://doi.10.1016/j.jhazmat.2020.122693

Eerkes-Medrano D, Thompson RC, Aldridge DC (2015) Microplastics in freshwater systems: a review of the emerging threats, identification of knowledge gaps and prioritisation of research needs. Water Res 75:63–82. https://doi.org/10.1016/j.watres.2015.02.012

Erni-Cassola G, Gibson MI, Thompson RC, Christie-Oleza JA (2017) Lost, but found with nile red: a novel method for detecting and quantifying small microplastics (1 mm to 20 μm) in environmental samples. Environ Sci Technol 51:13641–13648. https://doi.org/10.1021/acs.est.7b04512

Ewerts H, Barnard S, Swanepoel A (2017) The impact of zeta potential changes on *Ceratium hirundinella* cell removal and the ability of cells to restore its natural surface charge during drinking water purification. RSC Adv 7:22433–22440. https://DOI.10.1039/C7RA01185G

Hildebrandt TM, Nunes Nesi A, Araújo WL, Braun HP (2015) Amino acid catabolism in plants. Mol Plant 8:1563–1579. http://doi.10.1016/j.molp.2015.09.005

Hirota T, Izumi M, Wada S, Makino A, Ishida H (2018) Vacuolar protein degradation via autophagy provides substrates to amino acid catabolic pathways as an adaptive response to sugar starvation in *Arabidopsis thaliana*. Plant Cell Physiol 59:1363–1376. http://doi.10.1093/pcp/pcy005

Izumi M, Hidema J, Makino A, Ishida H (2013) Autophagy contributes to nighttime energy availability for growth in Arabidopsis. Plant Physiol 161:1682–1693. http://doi.10.1104/pp.113.215632

Jacques S, Ghesquière B, De Bock PJ, Demol H, Wahni K, Willems P, Messens J, Van Breusegem F, Gevaert K (2015) Protein methionine sulfoxide dynamics in *Arabidopsis thaliana* under oxidative stress. Mol Cell Proteomics 14:1217–1229. http://doi.10.1074/mcp.M114.043729

Kim YJ, Lee J, Park S, Park C, Park C, Chio HJ (2017) Effect of the relative permittivity of oxides on the performance of triboelectric nanogenerators. RSC Adv 78:49368–49373. http://dx.doi.org/10.1039/c7ra07274k

Li C, Busquets R, Campos LC (2019) Assessment of microplastics in freshwater systems: A review. Sci Total Environ (Epub ahead of print). https://doi.org/10.1016/j.scitotenv.2019.135578

Li WC, Tse HF, Fok L (2016) Plastic waste in the marine environment: A review of sources, occurrence and effects. Sci Total Environ 566–567:333–349. https://doi.org/10.1016/j.scitotenv.2016.05.084

Liu Q, Gao T, Liu W, Liu Y, Zhao Y, Liu Y, Li W, Ding K, Ma F, Li C (2020) Functions of dopamine in plants: a review. Plant Signal Behav 15:1827782. http://doi.10.1080/15592324.2020.1827782

Liu S, Hua T, Luo X, Lam NY, Tao X, Li L, Chio HJ (2015) A novel approach to improving the quality of chitosan blended yarns using static theory. Text Res J 85:1022–1034. https://doi.org/10.1177%2F0040517514559576

Lorenzen CJ (1967) Determination of chlorophyll and pheo-pigments: spectrophotometric equations 1. Limnol Oceanogr 12:343–346. https://doi.org/10.4319/lo.1967.12.2.0343

Mao Y, Ai H, Chen Y, Zhang Z, Zeng P, Kang L, Li W, Gu W, He Q, Li H (2018) Phytoplankton response to polystyrene microplastics: Perspective from an entire growth period. Chemosphere 208:59–68. https://doi.org/10.1016/j.chemosphere.2018.05.170

Masi A, Trentin AR, Agrawal GK, Rakwal R (2015) Gamma-glutamyl cycle in plants: a bridge connecting the environment to the plant cell? Front Plant Sci 6:252. http://doi.10.3389/fpls.2015.00252

Mintenig SM, Int-Veen I, Löder MGJ, Primpke S, Gerdts G (2017) Identification of microplastic in effluents of waste water treatment plants using focal plane array-based micro-Fourier-transform infrared imaging. Water Res 108:365–372. https://doi.org/10.1016/j.watres.2016.11.015

Monteleone A, Schary W, Fath A, Wenzel F (2019) Validation of an extraction method for microplastics from human materials. Clin Hemorheol Microcirc 73:203–217. https://doi.10.3233/CH-199209

Mubeen U, Jüppner J, Alpers J, Hincha DK, Giavalisco P (2018) Target of rapamycin inhibition in *Chlamydomonas reinhardtii* triggers de novo amino acid synthesis by enhancing nitrogen assimilation. Plant Cell 10:2240–2254. http://doi.10.1105/tpc.18.00159

NIES collection (2001) Media list, 1. Media for freshwater, terrestrial, hot spring and salt water algae. https://mcc.nies.go.jp/02medium-e.html

Nolte TM, Hartmann Nanna BJ, Kleijn M, Garnæs J, van de Meent D, Hendriks AJ, Baun A (2017) The toxicity of plastic nanoparticles to green algae as influenced by surface modification, medium hardness and cellular adsorption. Aquat Toxicol 183:11–20. https://doi.10.1016/j.aquatox.2016.12.005

OECD guidelines for the testing of chemicals, test no. 201: Freshwater alga and cyanobacteria, growth inhibition test 2011, 1–25. https://doi.org/10.1787/9789264069923-en

Ohashi Y, Hirayama A, Ishikawa T, Nakamura S, Shimizu K, Ueno Y, Tomita M, Soga T (2008) Depiction of metabolome changes in histidine-starved *Escherichia coli* by CE-TOFMS. Mol Biosyst 4:135–147. http://doi.10.1039/b714176a

Ohkama-Ohtsu N, Oikawa A, Zhao P, Xiang C, Saito K, Oliver DJ (2008) A gamma-glutamyl transpeptidase-independent pathway of glutathione catabolism to glutamate via 5-oxoproline in *Arabidopsis*. Plant Physiol. 148:1603–1613. http://doi.10.1104/pp.108.125716

Ooga T, Sato H, Nagashima A, Sasaki K, Tomita M, Soga T, Ohashi Y (2011) Metabolomic anatomy of an animal model revealing homeostatic imbalances in dyslipidaemia. Mol Biosyst 7:1217–1223. http://doi.10.1039/c0mb00141d

Prata JC, da Costa JP, Lopes I, Duarte AC, Rocha-Santos T (2019) Effects of microplastics on microalgae populations: A critical review. Sci Total Environ 665:400–405. https://doi.org/10.1016/j.scitotenv.2019.02.132

Qiao R, Sheng C, Lu Y, Zhang Y, Ren H, Lemos B (2019) Microplastics induce intestinal inflammation, oxidative stress, and disorders of metabolome and microbiome in zebrafish. Sci Total Environ 662:246–253. http://doi.10.1016/j.scitotenv.2019.01.245

Rezania S, Park J, Md Din MF, Mat Taib S, Talaiekhozani A, Kumar Yadav K, Kamyab H (2018) Microplastics pollution in different aquatic environments and biota: A review of recent studies. Mar Pollut Bull 133:191–208. https://doi.org/10.1016/j.marpolbul.2018.05.022

Ruiz RR, Martinez F, Beiter GK (2019) The effects of GABA in plants. Cogent Food Agric 5:1670553. https://doi.org/10.1080/23311932.2019.1670553

Sjollema SB, Redondo-Hasselerharm P, Leslie HA, Kraak MHS, Vethaak AD (2016) Do plastic particles affect microalgal photosynthesis and growth? Aquat Toxicol 170:259–261. https://doi.org/10.1016/j.aquatox.2015.12.002

Scopetani C, Chelazzi D, Cincinelli A, Esterhuizen-Londt M (2019) Assessment of microplastic pollution: occurrence and characterisation in Vesijärvi Lake and Pikku Vesijärvi Pond, Finland. Environ Monit Assess 191:652. https://doi.10.1007/s10661-019-7843-z

Shevyakova NI, Rakitin VY, Duong DB, Sadomov NG, Kuznetsov VV (2001) Heat shock-induced cadaverine accumulation and translocation throughout the plant. Plant Sci 161:1125–1133. https://doi.org/10.1016/S0168-9452(01)00515-5

Song C, Liu Z, Wang C, Li S, Kitamura Y (2020) Different interaction performance between microplastics and microalgae: The bio-elimination potential of *Chlorella* sp. L38 and *Phaeodactylum Tricornutum* MASCC-0025. Sci Total Environ 723:138146. https://doi.10.1016/j.scitotenv.2020.138146

Sugimoto M, Wong DT, Hirayama A, Soga T, Tomita M (2009) Capillary electrophoresis mass spectrometry-based saliva metabolomics identified oral, breast and pancreatic cancer–specific profiles. Metabolomics 6:78–95. http://doi.10.1007/s11306-009-0178-y

Teng J, Zhao J, Zhu X, Shan E, Zhang C, Zhang W, Wang Q (2021) Toxic effects of exposure to microplastics with environmentally relevant shapes and concentrations: Accumulation, energy metabolism and tissue damage in oyster *Crassostrea gigas*. Environ Pollut 269:116169. http://doi.10.1016/j.envpol.2020.116169

Timm K, Myant C, Spikes HA, Grunze M (2011) Particulate lubricants in cosmetic applications. Tribol Int 44:1695–1703. https://dx.doi.org/10.1016/j.triboint.2011.06.017

Thompson RC, Olsen Y, Mitchell RP, Davis A, Rowland SJ, John AW, McGonigle D, Russell AE (2004) Lost at sea: where is all the plastic? Science 304:838. https://doi.org/10.1126/science.1094559

Wagner J, Wang ZM, Ghosal S, Murphy M, Wall S, Cook AM, Robberson W, Allen H (2019) Nondestructive extraction and identification of microplastics from freshwater sport fish stomachs. Environ Sci Technol 53:14496–14506. https://doi.10.1021/acs.est.9b05072

Wu X, Liu Y, Yin S, Xiao K, Xiong Q, Bian S, Liang S, Hou H, Hu J, Yang J (2020) Metabolomics revealing the response of rice (*Oryza sativa* L.) exposed to polystyrene microplastics. Environ Pollut 266 (Pt 1):115159. http://doi.10.1016/j.envpol.2020.115159

Yan M, Nie H, Xu K, He Y, Hu Y, Huang Y, Wang J (2019) Microplastic abundance, distribution and composition in the Pearl River along Guangzhou City and Pearl River Estuary, China. Chemosphere 217:879–886. https://doi.10.1016/j.chemosphere.2018.11.093

Yi X, Chi T, Li Z, Wang J, Yu M, Wu M, Zhou H (2019) Combined effect of polystyrene plastics and triphenyl tin chloride on the green algae *Chlorella pyrenoidosa*. Environ Sci Pollut Res 26:15011–15018. https://doi.org/10.1007/s11356-

019-04865-0

Zhang C, Chen X, Wang J, Tan L (2017) Toxic effects of microplastic on marine microalgae *Skeletonema costatum*: Interactions between microplastic and algae. Environ Pollut 220 (Pt B):1282–1288. http://doi.10.1016/j.envpol.2016.11.005

Zhu ZL, Wang SC, Zhao FF, Wang SG, Liu FF, Liu GZ (2019) Joint toxicity of microplastics with triclosan to marine microalgae *Skeletonema costatum*. Environ Pollut 246:509–517. http://doi.10.1016/j.envpol

Figures

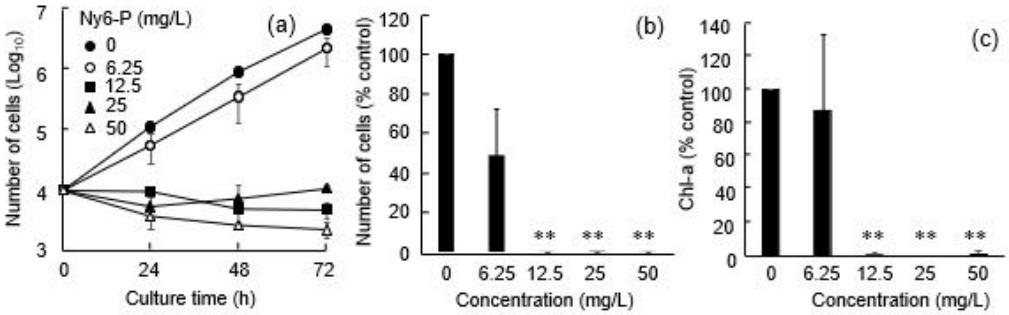

Figure 1

Effects of powdered nylon 6 (Ny6-P) on Raphidocelis subcapitata (a) Growth dynamics of R. subcapitata with exposure to Ny6-P at concentrations of 6.25, 12.5, 25, and 50 mg/L for 72 h. (b) cell numbers and (c) chlorophyll-a (Chl-a) contents after the same exposure. Data are shown as mean ± standard deviation. * and ** represent significant differences relative to the controls at $P < 0.05$ and $P < 0.01$, respectively.

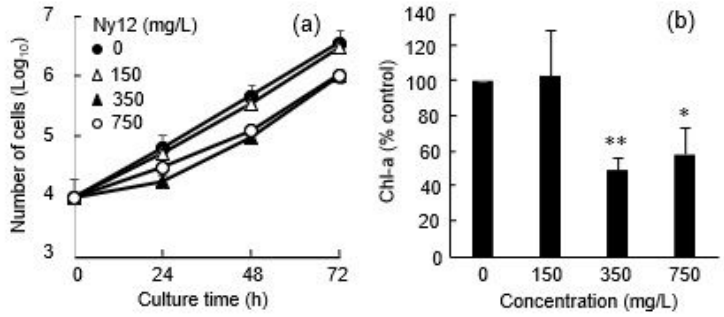

Figure 2

Effects of nylon 12 (Ny12) on Raphidocelis subcapitata (a) Growth dynamics and (b) chlorophyll-a (Chl-a) contents after exposure of R. subcapitata to Ny12 at concentrations of 150, 350, and 750 mg/L for 72 h. Data are shown as mean ± standard deviation. * and ** represent significant differences relative to the controls at $P < 0.05$ and $P < 0.01$, respectively.

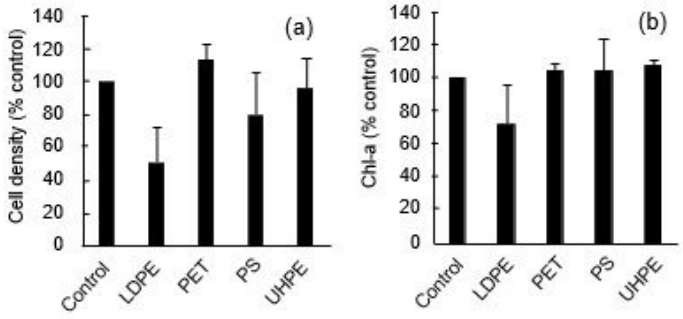

Figure 3

Effects of four powdered microplastics (MPs) on Raphidocelis subcapitata Comparison of (a) cell numbers and (b) chlorophyll-a (Chl-a) contents of R. subcapitata exposed to low-density polyethylene (LDPE), PE terephthalate (PET), polystyrene (PS), and ultra-high-molecular-weight PE (UHPE) at 750 mg/L for 72 h. Error bars represent standard deviations.

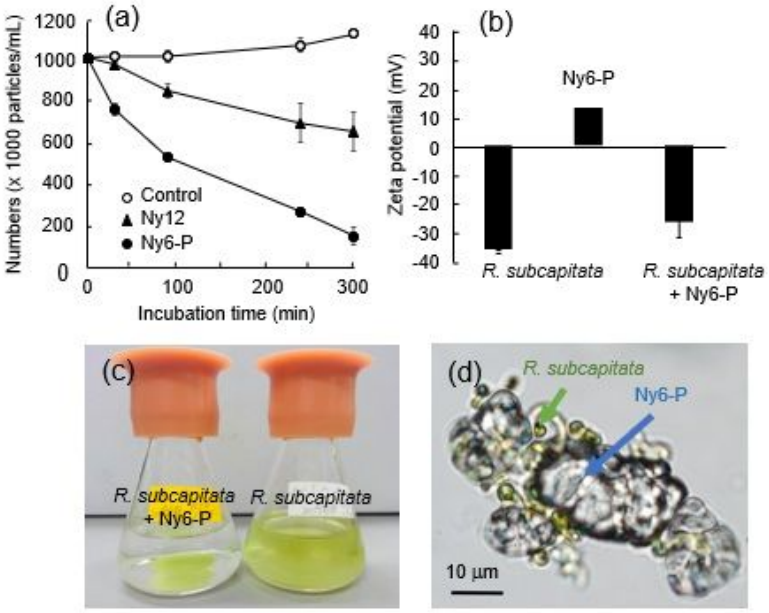

Figure 4

Nylon particle adhesion of Raphidocelis subcapitata cells (a) Dynamics of algal cells treated with powdered nylon 6 (Ny6-P) or nylon 12 (Ny12) in culture supernatants. (b) Zeta potential of R. subcapitata, Ny6-P, and R. subcapitata mixed with Ny6-P (R. subcapitata + Ny6-P). (c) Culture media containing R. subcapitata in flasks after 300 min of stirring with or without Ny6-P treatment. (d) Micrograph of Ny6-P adhering to R. subcapitata cells.

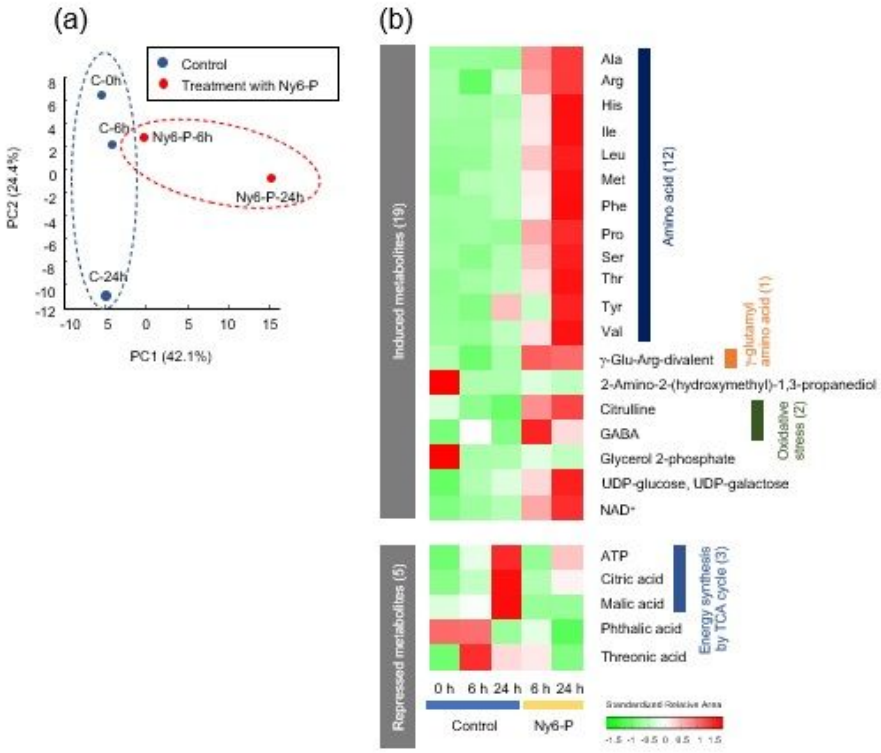

Figure 5

Metabolomic alterations in Raphidocelis subcapitata after exposure to Ny6-P (a) Principal component analysis (PCA) plots of metabolite profiles from R. subcapitata treated with Ny6-P. The percentages listed on the axis labels indicate the fraction of variance explained by the first (PC1) and second (PC2) principal components. Ny6-P-6h and Ny6-P-24h show plots of R. subcapitata treated with Ny6-P for 6 and 24 h, respectively. C-0h, C-6h, and C-24h show plots of R. subcapitata without Ny6-P (control) incubated for 0, 6, and 24 h, respectively. (b) Metabolic alterations of R. subcapitata treated with Ny6-P. The heatmap shows induced or repressed metabolites in P. subcapitata cells exposed to Ny6-P for 6 and 24 h.

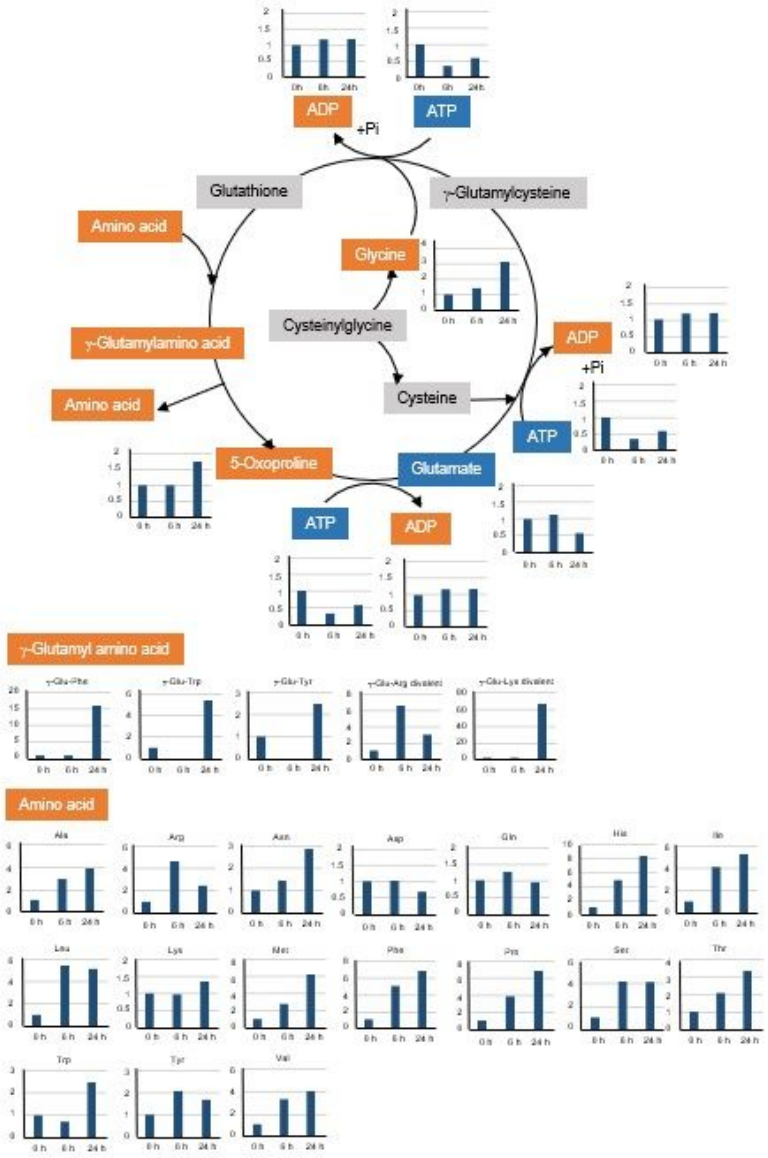

Figure 6

Metabolites related to the γ-glutamyl cycle in Raphidocelis subcapitata after exposure to Ny6-P Orange, induced; blue, repressed; gray, not detected. Vertical axes show fold changes of metabolites in R. subcapitata cells treated with Ny6-P compared with the control.

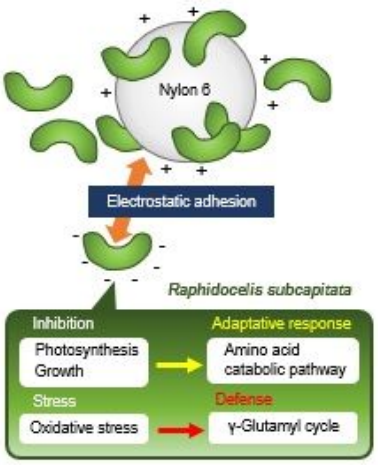

Figure 7

A model diagram of the interaction mechanism between Raphidocelis subcapitata and Ny6-P

Supplementary Files

This is a list of supplementary files associated with this preprint. Click to download.

- SupplementarydataFigMizukamiMurata210318.pptx
- SupplementarydataTableMizukamiMurata210318.docx